

# Menstrual Cycle Heat Maps

## Visualising menstrual cycle variability using hormone heat map arrays referenced to the ultrasound day of ovulation

Thomas P. Bouchard<sup>1</sup>, Saman H. Abdulla<sup>2</sup>, Rene Leiva<sup>3,4</sup>, René Ecochard<sup>5,6,7,8</sup>

<sup>1</sup>Department of Family Medicine, University of Calgary, Calgary, Alberta, Canada; <sup>2</sup>Department of Statistics and Information, College of Administration and Economics, University of Sulaimani, Sulaimani, Iraq. <sup>3</sup>Bruyère Research Institute, CT Lamont Primary Health Care Research Centre, Ottawa, Ontario, Canada; <sup>4</sup>University of Ottawa, Department of Family Medicine, Ottawa, Ontario, Canada; <sup>5</sup>Hospices Civils de Lyon, Service de Biostatistique-Bioinformatique, Lyon, France. <sup>6</sup>Université de Lyon, Lyon, France; <sup>7</sup>Université Lyon 1, Villeurbanne, France; <sup>8</sup>CNRS, Laboratoire de Biométrie et Biologie Evolutive, Equipe Biostatistique-Santé, Villeurbanne, France

<https://doi.org/10.63264/qk8aw674>

### ABSTRACT

**Background:** There is considerable individual day-to-day variation within the menstrual cycle and between cycles in women. Average hormone curves inadequately describe the individual hormone patterns experienced by women.

**Objective:** The present study applies a novel application (proof-of-concept) of a statistical array (heat map) to show both individual and group menstrual cycle hormone variability.

**Design:** Using pre-existing datasets, two cohorts of women were analysed using a statistical method to visualise quantitative hormonal variation.

**Subjects:** In one cohort, 107 women contributed a total of 283 menstrual cycles and in the second cohort, 21 women contributed a total of 62 menstrual cycles.

**Method:** Women collected first morning urine samples for analysis of estrone-3-glucuronide (E1G) and luteinizing hormone (LH) in both datasets. In the larger dataset, pregnanediol-3-alpha-glucuronide (PDG) and follicle-stimulating hormone (FSH) were also collected. Serial ultrasounds identified the precise day of ovulation in the larger dataset. In the smaller dataset, peak LH was used to identify the estimated day of ovulation.

**Outcome measure:** The main outcome measure was to visualise hormonal variability using hormone array heat maps.

**Conclusion:** Heat maps were able to quickly show clustering of hormone patterns in the fertile window and on the day of ovulation. Individual differences were identified in rows on the heat map relative to the day of ovulation. This new tool to visually represent hormonal changes with heat maps identifies both individual and group variability of menstrual cycle hormones.

**Keywords:** menstrual cycle; luteinizing hormone; estrone-3 glucuronide; pregnanediol-3 glucuronide; ovulation; heat maps

### INTRODUCTION

Until the end of the twentieth century, precise characterisation of hormonal profiles of the menstrual cycle was limited. It was common to use average approximate curves to represent hormonal patterns. This “textbook” approach to visualising the menstrual cycle created an impression that day to day variation in hormones was somehow abnormal. The availability of repeated hormone assays throughout a woman's cycle has revealed a great diversity of profiles, both between cycles and between women.<sup>1-6</sup> Since these quantitative hormone assays are now readily available,<sup>7-11</sup> individual hormone profiles need to be evaluated and new methods of visualising these variations are needed. Attempts have been made to show daily variation in menstrual cycle hormones, but have not been able to simultaneously describe both individual and group variability.<sup>7,12,13</sup>

Previous studies have demonstrated possible distributions of hormones using statistical modelling, specifically a beta-binomial distribution to describe specific patterns in the daily hormone changes of luteinizing hormone (LH) and pregnanediol glucuronide (PDG).<sup>14</sup> In the figures in that study, the statistical fit line was shown with a background of individual hormone profiles (see Figures 2 and 3 in this study), however these individual profiles are not discernible when plotted together.

There is a need to develop new visualisation tools to show both individual and group variability in quantitative menstrual cycle hormones. This requires statistical tools that can represent a large amount of quantitative data. Other fields, notably

Received February 6, 2025; revised April 10, 2025; accepted April 13, 2025.

© The Author(s) 2025. Published by The Journal of Restorative Reproductive Medicine. This is an Open Access article distributed under the terms of the Creative Commons Attribution License (<https://creativecommons.org/licenses/by/4.0/>), which permits unrestricted reuse, distribution, and reproduction in any medium, provided the original work is properly cited.

genomics, facing the same proliferation of information, have turned to heat maps to represent data.<sup>15</sup> The use of heat maps<sup>16</sup> could open new avenues in the study of menstrual cycle hormonal profiles in both physiological and pathological situations. In the genetic context, heat maps display data in a grid, where each row can represent a sample and each column can represent a gene, or vice versa. The colour and intensity of the boxes are used to represent gene expression. On a graph, the diversity of gene expression can be seen at a glance. Several authors have documented a range of hormonal profiles in normally fertile women, noting that there is a continuum from normal to abnormal cycles.<sup>1-6</sup> Heat maps could facilitate the study of this diversity.

It is also common to visualise clusters with heatmaps.<sup>17</sup> The use of such methods may offer a new way to identify subgroups of women with similar hormonal profiles, for example in the context of infertility or polycystic ovarian syndrome (PCOS).<sup>18</sup> It could also be used to identify factors associated with physiological luteal phase diversity in hormone profiles (especially progesterone) and thus the likelihood of successful implantation. In the present study, we will present examples of heat maps of hormonal profiles during the menstrual cycle, illustrating the possibility of representing hundreds of individual profiles in a single array, where group and individual variability can simultaneously be visualised.

This study used the Quidel menstrual cycle database<sup>19</sup> and a pilot database of Mira monitor urine hormone results.<sup>7</sup> The Quidel database was collected from regularly menstruating women in the 1990s and has previously been used to study the fertile window. The Mira pilot study compared the use of the ClearBlue Fertility Monitor to the Mira Monitor in identifying ovulation. While the Quidel database is referenced to the ultrasound estimate of the day of ovulation, the Mira monitor was referenced only to the ClearBlue monitor's estimated day of ovulation (which itself has been referenced to the ultrasound day of ovulation). The aim of this study was to develop a proof-of-concept visual array (heatmap) of hormones to demonstrate individual and group variability in the menstrual cycle.

## METHODS

### Subjects

The Quidel subjects of this prospective cohort study, described in detail elsewhere,<sup>19</sup> were approached in the mid-1990s in eight natural family planning centres in five European countries: France, Italy, Germany, Belgium and Spain. Subjects were informed of the purpose of the study. They were also informed that they could withdraw at any time. All participants gave written informed consent, and the study procedures were conducted in accordance with the ethical standards for human experimentation set out in the Declaration of Helsinki. Inclusion criteria were healthy women aged 18-45 years with a previous menstrual cycle of 24-34 days. Subjects were excluded if they were breastfeeding, postpartum (first 3 months) or perimenopausal; had frequent anovulatory cycles; were on fertility hormone stimulation programmes; or had abnormal

cycles (PCOS, luteal defect), pelvic inflammatory disease, a history of fertility problems, or special habits such as running.

The Mira monitor pilot<sup>7</sup> participants were recruited to compare Mira monitor quantitative hormone results to ClearBlue monitor Low, High and Peak results, both measuring E1G and LH in the urine at home. Ethics approval was obtained from the Health Research Ethics Board of Alberta, and all participants signed a witnessed consent. Inclusion criteria were healthy women aged 18-42 years with regular cycles (<7 days variation between cycles) ranging between 21-42 days. Subjects were excluded if they were on medication that affected ovulation within 3 months, currently pregnant or breastfeeding, or having fertility problems (PCOS, endometriosis, other infertility).

### Ultrasound scans

In the Quidel cohort, serial transvaginal ovarian ultrasounds (with follicle measurements) commenced either at the onset of fertile cervical mucus, as observed or felt by the woman at the vulva, or upon detection of the LH surge using a home test (Quidel Corporation, San Diego, CA). These scans were performed every other day until the largest follicle reached 16 mm, followed by daily scans until ovulation was confirmed. The estimated day of ovulation as determined by ultrasound (USDO) was defined as the day of maximum follicular enlargement followed the next day by evidence of rupture.

### Urine hormone measurements

For the Quidel cohort, first morning urine was tested with Quidel at home LH tests and urine specimens were also collected and frozen and later assayed for E1G and PDG using Delfia time-resolved fluorometric immunosorbent assays. In this dataset the assays were tested in duplicates and adjusted for creatinine.

For the Mira cohort, first morning urine was tested by each participant on the Mira monitor and included both E1G (ng/mL) and LH (mIU/mL) quantitative hormone results. The Mira monitor uses a fluorescence assay that has been described in detail in previous studies.<sup>20</sup> In this dataset, creatinine adjustments were not done.

### Statistical analysis

In the Quidel cohort, the analysis was restricted to cycles with a clearly defined ultrasound-determined day of ovulation (US-DO). Data associated with potential pregnancies (luteal phase longer than 17 days) were excluded. For the Mira cohort, ultrasound was not included but the day of ovulation was referenced to the ClearBlue day of ovulation which has an established correlations with the US-DO, i.e. ovulation occurred on one of the two ClearBlue peak days 91% of the time,<sup>21</sup> and the Mira LH peak occurred on one of the two ClearBlue peak days 86% of the time,<sup>7</sup> which makes the Mira LH peak day a reasonable approximation for the US-DO. Using R software (version 4.3.2), heat maps were used to visualise hormone arrays, where rows represent different individuals' data and columns represent the day relative to ovulation. Colour

intensity represents hormone levels, with different colours or shades indicating different concentrations of hormones. The term “signal” is referenced throughout the manuscript to indicate a quantitative hormonal change that can be interpreted relative to the surrounding “noise,” i.e. an observable and repeatable pattern (in this case visual) in each hormone profile.

**RESULTS**

**Demographics**

In the Quidel cohort, there were 107 women who contributed 283 cycles for analysis. They were 19–45 years old with menstrual cycle lengths of 24–34 days. In the Mira cohort, there were 21 women who contributed 62 cycles for analysis. They were 23–42 years old, with cycle lengths of 23–41 days.

**Average hormone curves**

In order to illustrate the information provided by an average hormone profile, the Quidel dataset was plotted in Figure 1, which shows the typical appearance of the menstrual cycle hormones that are frequently reported in textbook diagrams of the menstrual cycle, but without representing individual variability.

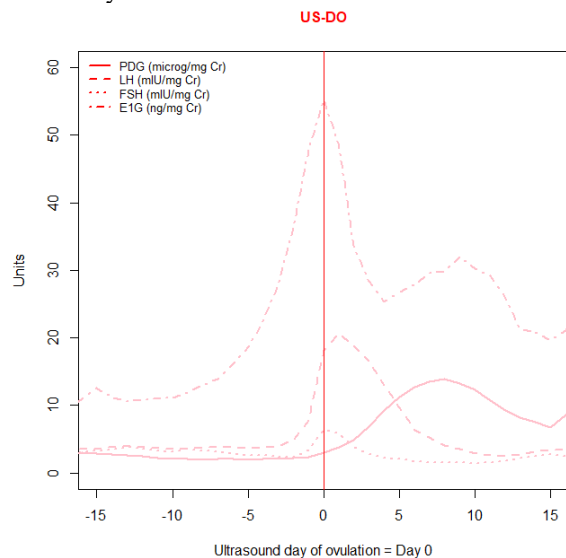


*Figure 1.* Average hormonal curves for follicle stimulating hormone (FSH), luteinizing hormone (LH), pregnanediol-3-glucuronide (PDG) and estrone-3-glucuronide (E1G) from the Quidel dataset.

**Average with individual hormone curves**

An alternative that has previously been used<sup>14</sup> shows individual and average hormone profiles for LH (Figure 2) and PDG (Figure 3) for the days before and after ovulation (Day 0), both from the Quidel dataset (reproduced with methods from our previous study<sup>14</sup>). However, the multiple individual profiles are not easily appreciated when plotted together.

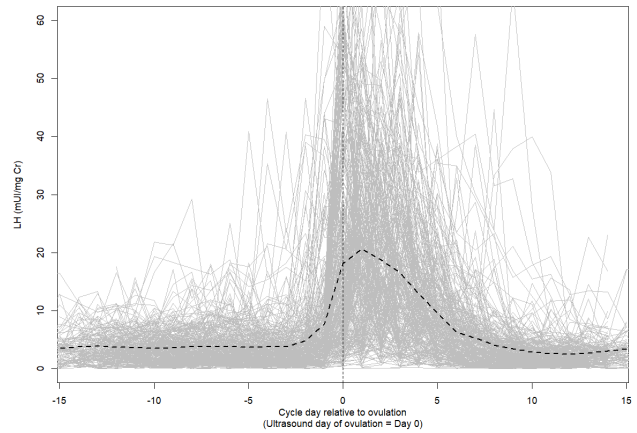


*Figure 2.* Luteinizing hormone (LH) profiles with statistical fit lines (dark line) on a background of individual LH profiles (grey lines). (A) and (B) are based on different beta-binomial parameters used to create the fit line. From the Quidel dataset, created using the same method as reference 14.

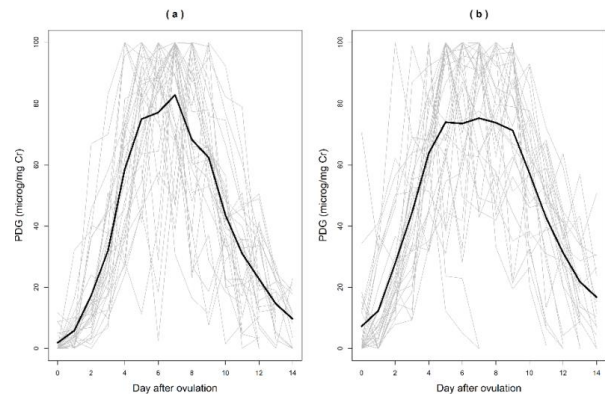


*Figure 3.* Progesterone (PDG) profiles with statistical fit lines (dark line) on a background of individual PDG profiles (grey lines). (A) and (B) are based on different beta-binomial parameters used to create the fit line. From the Quidel dataset, created using the same method as reference 14.

**LH hormone heat maps**

Heat maps can simultaneously show individual and group patterns of each hormone. The distribution of luteinizing hormone surge can be seen in both datasets concentrated around the day of ovulation (Figure 4). In the Quidel dataset, individual variation can be seen where an increased or prolonged LH signal is seen in the 3–4 days after the estimated day of ovulation (EDO = day 0). In the Mira dataset, most of the LH surge signal is seen on the day before the estimated day of ovulation, and the day of the estimated day of ovulation (day 0). In both datasets, outliers can be seen with elevated LH levels outside the expected time of ovulation.

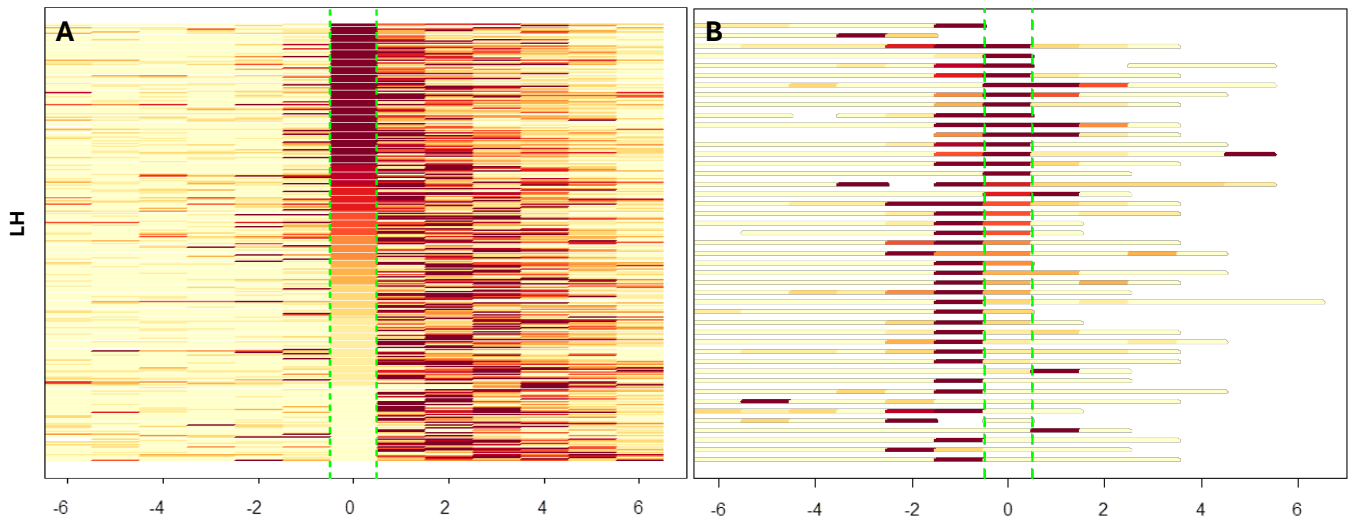


*Figure 4.* LH hormone arrays in the Quidel cohort (A) and the Mira cohort (B). Concentration of LH patterns are around the estimated day of ovulation in both cases, but in the Quidel cohort, there is far more LH signal after the US-DO, and in the Mira cohort, the high LH is concentrated both on the day before the estimated day of ovulation and on the estimated day of ovulation, i.e. the LH-DO which is the LH peak.

**E1G hormone heat maps**

The E1G signal in both cases can be seen rising (darker intensity lines) leading up to the EDO (Figure 5). These hormone arrays also show that there may be differences

between the assays, with an increase in E1G slightly earlier in the Mira cohort (Figure 5B) than in the Quidel cohort.

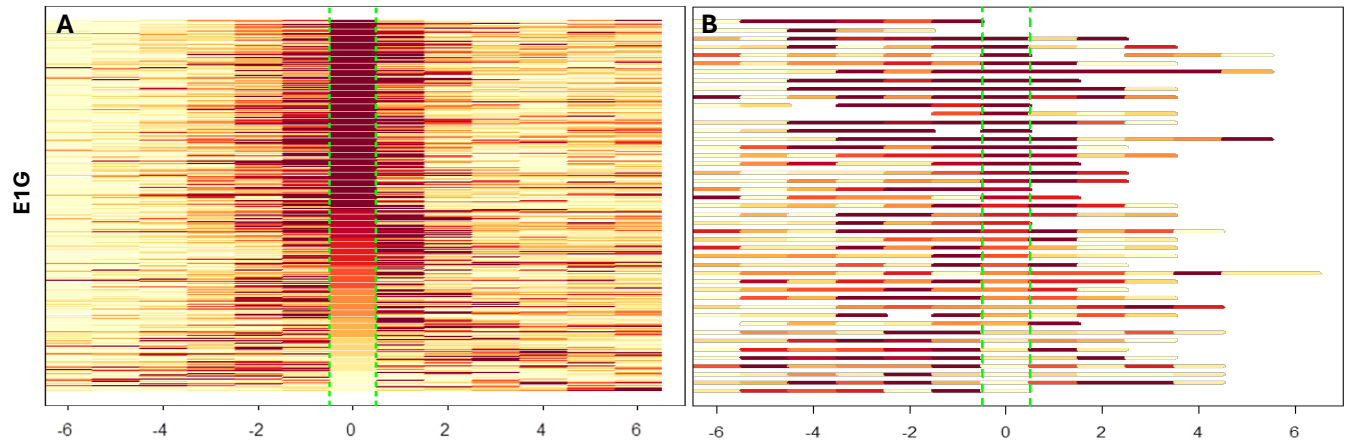


*Figure 5.* E1G hormone arrays in the Quidel cohort (A) and the Mira cohort (B). Concentration of E1G patterns, like LH, are around the estimated day of ovulation in both cases. E1G has a greater signal before the EDO. In the Quidel cohort (A), the E1G signal begins 3-4 days before the EDO (US-DO). In the Mira cohort (B), the E1G signal begins 4-5 days before the EDO (LH-DO). The E1G patterns also continues in the 2 days after the EDO in both cohorts as well.

**FSH and PDG hormone heat maps**

Only the Quidel dataset included FSH and PDG measurements, as shown in Figure 6. An FSH signal (rise) is clearly observed around the EDO, with some changes in the follicular phase. A broader window of days around the EDO (Figure 7) still does not show a clear pattern for FSH,

suggesting greater individual variability between cycles for FSH. The pattern for PDG, on the other hand, is clearly concentrated in the luteal phase (from EDO to the end of the cycle), rising a few days after the EDO and staying elevated as shown in Figure 6B and 7D.

**Visualizing menstrual cycle dynamics by heat maps per hormone**

The pattern changes in all four menstrual cycle hormones (FSH, E1G, LH and PDG) can be seen in the Quidel dataset (Figure 7) referenced to the ultrasound day of ovulation. In this case a broader span of the menstrual cycle (from 12 days before ovulation, day 0, to 12 days after ovulation) shows the dynamic interplay between the four hormones as the cycle evolves. In the follicular phase, the FSH signal (Figure 7A) precedes changes in E1G (Figure 7B) prior to ovulation (EDO = 0). The LH signal is concentrated on the day of ovulation and the 1-3 days after ovulation (Figure 7C). As the LH signal decreased, PDG starts to rise and stays

elevated throughout the luteal phase (Figure 7D).

The E1G signal (7B) begins in the late follicular phase (day -3) and continues throughout the luteal phase.

The LH signal (7C) begins mainly on the day of ovulation (EDO) but does not always have a narrow signal isolated to that day but in some cases has a broader signal that continues into the early luteal phase.

PDG (7D) clearly has a luteal phase distribution, and the rise on EDO+3, peak around EDO+7 and fall on EDO+12 can clearly be seen on this heat map.

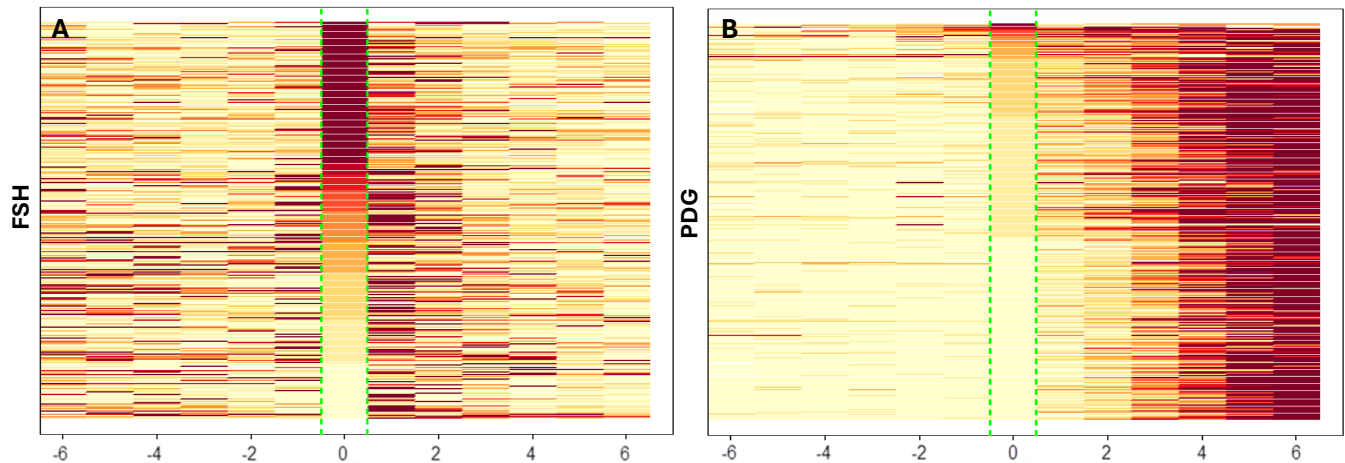


*Figure 6.* FSH hormone arrays (A) and PDG hormone arrays (B) in the Quidel cohort show that the distribution of FSH signal is quite broad, with an increase in FSH around the EDO, but a scattered signal in the follicular phase. On the other hand, the PDG signal is clearly in the luteal phase after the EDO, as would be expected physiologically.

## DISCUSSION

Although heat maps<sup>16</sup> have been widely employed in genomics,<sup>17,18</sup> to our knowledge they have not yet been used to represent the hormones of the menstrual cycle. Many studies have shown the importance of individual variability in menstrual cycles,<sup>6,12,13,22</sup> but to date there have not been adequate methods to visualize both individual and group changes in hormone patterns. In the present study we have shown that this visualizing menstrual cycle hormones with heat maps can be employed to better understand the menstrual cycle in two separate datasets, with different assays for E1G and LH.

The beginning of the fertile window, which has been theoretically established based on sperm survival as 6 days up to and including the day of ovulation,<sup>23</sup> is difficult to

precisely delineate with a single hormone threshold change. Although attempts to identify the beginning of the fertile window have been made,<sup>24</sup> applying complex algorithms may be difficult to incorporate into specific methods to achieve or avoid pregnancy. Identifying the beginning of the fertile window in the two datasets presented here remains elusive. In Figure 5 and 7B, the E1G rise certainly occurs in the 3-5 days prior to ovulation but this is not a uniform finding, in many cases E1G only rises 1 or 2 days prior to ovulation (as seen by looking at individual rows in these figures). One might also expect to find a clear signal in FSH, where it decreases prior to the onset of the fertile window, but this pattern is also not uniform across cycles as shown in Figures 6A and 7A and so its use as a predictor of the onset of the fertile window may not be promising.

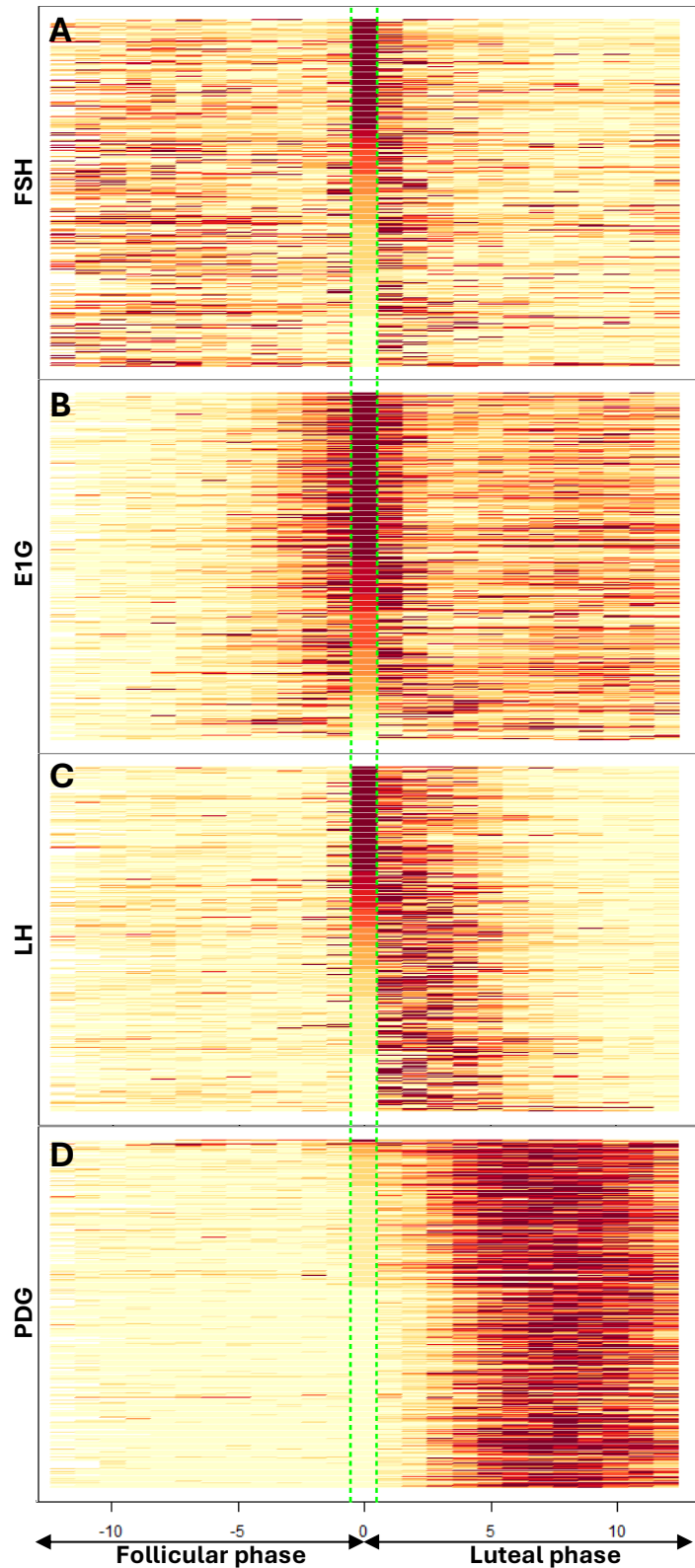


*Figure 7.* Quidel dataset showing dynamic progression in hormone patterns with specific hormone concentrations in the follicular phase (FSH and E1G, A and B), around the time of ovulation (E1G and LH, B and C) and in the luteal phase – in the early luteal phase for LH (C), a subtle signal throughout the luteal phase for E1G (B), and a strong signal for PDG rising to a plateau (D).

The prediction of ovulation using E1G and LH has been reliably implemented by many fertility monitors, including the ClearBlue monitor,<sup>21</sup> but more modern quantitative monitors like Mira,<sup>7</sup> Inito,<sup>8</sup> Proov,<sup>9</sup> and Oova,<sup>11</sup> have not been validated to the gold standard of ultrasound-confirmed ovulation, so their specific ability to predict the precise day of ovulation remains to be established.<sup>20</sup> If future studies show that these monitors accurately predict ovulation, the use of heat maps as shown here to visualise their models may be useful in analysing their assays' temporal relationship to ovulation. It should be noted, however, that self-observation cervical mucus has been shown to identify the clinical fertile window and ovulation but there is also variability in this observation as well.<sup>25</sup>

Although the LH surge has been used to identify ovulation, there are several observations worth noting in the present study and in previous studies. First, the LH surge may not always follow the expected sharp rise and fall (i.e. a one day LH surge), and previous work on the Quidel dataset has shown a diversity of LH patterns in relation to ovulation.<sup>13</sup> This was shown visually in Figure 4A and 7C in the Quidel cohort, specifically that the LH rise is not isolated to the ultrasound EDO (Day 0) but may last over 3-4 days. It is important to note that the LH rise or surge (not just the highest, or "peak," day) is important to consider relevant to the day of ovulation,<sup>13</sup> since it can be seen in some cases in the Quidel dataset that ovulation occurs with the rise in LH, but before the peak LH levels (Figure 2 and Figure 4). The finding of the LH surge but not the peak happening before the day of ovulation has previously been described in the Quidel data.<sup>19</sup> The different luteinization patterns may also impact the later evolution of the progestation process and may delay PDG results as we have previously suggested.<sup>12</sup> Interestingly, the Mira cohort (Figure 4B) showed a narrower LH surge over the day before and the day of predicted ovulation with only a few outliers on days outside of these. However, this difference between the two datasets may simply be the effect of an artifact: using the LH peak day as the reference day for the Quidel dataset, the same narrower LH surge is obtained over the day before and the day of predicted ovulation. Moreover, the Quidel and Mira, despite measuring the same hormone, are different assays, therefore there may be differences related to the assays themselves. Importantly, the heat maps allow for easy identification of outliers among the cohorts outside of the expected days for LH changes but also visualising differences between different LH assays. Visualising LH outliers with heat maps may be useful in other situations like the postpartum and perimenopause fertility transitions, where multiple LH rises may be seen because a higher LH threshold is required to trigger ovulation, as was previously shown.<sup>26</sup>

In the luteal phase, the findings of a rise, plateau, peak and fall in PDG is no surprise. The Quidel dataset findings in the luteal phase have been well described,<sup>6,12,27</sup> but importantly, the heat maps have demonstrated the expected luteinization (rise in progesterone), progestation (plateau of progesterone and peak at EDO+7), and luteolysis (decrease in

progesterone at EDO+12) which we have described physiologically in our previous work.<sup>6</sup> What is of additional interest is the findings of E1G signal as it suggests luteal follicular activity. In Figure 7B, there are higher levels of E1G than in the early to mid-follicular phase, reflecting estrogen secretion by the corpus luteum. Some authors have suggested that this secretion may also be due in part to the preparation of follicles that begins in the luteal phase of the previous cycle.<sup>28</sup> This concentration of E1G changes appears to be greater even than FSH changes in the luteal phase.

The main strengths of the current study are the application of the visual hormone arrays (heat maps) in two different cohorts which provide different insights based on the assay results. In the larger Quidel cohort, the estimated day of ovulation was based on ultrasound (US-DO), which is the gold-standard for identifying ovulation. One weakness was the smaller sample size in the Mira cohort and that this group's estimated day of ovulation was referenced to an established day of ovulation from another monitor (ClearBlue). Although the current study was not meant to statistically compare the two groups, since it was mainly a proof-of-concept demonstration of a new tool for visualising menstrual cycle hormone variability within and between cycles, future studies could analyse the statistical differences between different hormone heat maps. Several statistical packages are now available to identify clusters in a series of measurements from multiple individuals. Some are dedicated to unordered measurements,<sup>29</sup> as is the case with genomic data for example, others take into account the rank of the measurements,<sup>30</sup> which seems more appropriate for hormonal data, with days being the order. Visualising the menstrual cycle with heat maps may help to improve menstrual health literacy among health care providers and their patients, giving them a better appreciation of the hormonal variability between women and from one cycle to the next.

## CONCLUSION

Visual hormone arrays (heat maps) of the menstrual cycle provide a clear visual representation of hormone fluctuations across the menstrual cycle, highlighting both the general trends and individual variability within and between cycles. This method of representing the menstrual cycles has many applications in evaluating normal and abnormal menstrual cycles, with the potential to improve our understanding of the hormonal dynamics associated with folliculogenesis, ovulation and the luteal phase.

## ACKNOWLEDGEMENT

The authors thank Drs. Sophie Dubus, Anne Leduy, Isabelle Ecochard, Marie Grisard Capelle, Enriqueta Barranco, Michele Barbato, Sandro Girotto, and Marion Gimmler from the Fertility Awareness Clinics as well as all the women who took part in this study.

**CONFLICT OF INTEREST DISCLOSURES**

T. Bouchard currently has a Mitacs grant that is co-sponsored by Mira (Quanovate Tech).

**FUNDING STATEMENT**

This study did not receive any funding.

**ETHICAL APPROVAL**

Study approvals and informed consent statements described in methods.

**DATA AVAILABILITY**

The authors can make anonymized data available based on request.

**REFERENCES**

1. Brown JB. Types of ovarian activity in women and their significance: the continuum (a reinterpretation of early findings). *Hum Reprod Update*. 2011 Mar-Apr;17(2):141-58. doi: [10.1093/humupd/dmq040](https://doi.org/10.1093/humupd/dmq040). Epub 2010 Oct 5.
2. Blackwell LF, Vigil P, Gross B, d'Arcangues C, Cooke DG, Brown JB. Monitoring of ovarian activity by measurement of urinary excretion rates of estrone glucuronide and pregnenediol glucuronide using the Ovarian Monitor, Part II: reliability of home testing. *Hum Reprod*. 2012 Feb;27(2):550-7. doi: [10.1093/humrep/der409](https://doi.org/10.1093/humrep/der409)
3. Schliep KC, Mumford SL, Hammoud AO, Stanford JB, Kissell KA, Sjaarda LA, Perkins NJ, Ahrens KA, Wactawski-Wende J, Mendola P, Schisterman EF. Luteal phase deficiency in regularly menstruating women: prevalence and overlap in identification based on clinical and biochemical diagnostic criteria. *J Clin Endocrinol Metab*. 2014 Jun;99(6):E1007-14. doi: [10.1210/jc.2013-3534](https://doi.org/10.1210/jc.2013-3534)
4. Allende ME. Mean versus individual hormonal profiles in the menstrual cycle. *Fertil Steril*. 2002 Jul;78(1):90-5. doi: [10.1016/s0015-0282\(02\)03167-9](https://doi.org/10.1016/s0015-0282(02)03167-9)
5. Park SJ, Goldsmith LT, Skurnick JH, Wojtczuk A, Weiss G. Characteristics of the urinary luteinizing hormone surge in young ovulatory women. *Fertil Steril*. 2007 Sep;88(3):684-90. doi: [10.1016/j.fertnstert.2007.01.045](https://doi.org/10.1016/j.fertnstert.2007.01.045)
6. Ecochard R, Bouchard T, Leiva R, Abdulla S, Dupuis O, Duterque O, Garmier Billard M, Boehringer H, Genolini C. Characterization of hormonal profiles during the luteal phase in regularly menstruating women. *Fertil Steril*. 2017 Jul;108(1):175-182.e1. doi: [10.1016/j.fertnstert.2017.05.012](https://doi.org/10.1016/j.fertnstert.2017.05.012)
7. Bouchard TP, Fehring RJ, Mu Q. Quantitative Versus Qualitative Estrogen and Luteinizing Hormone Testing for Personal Fertility Monitoring. *Expert Rev Mol Diagn*. 2021;21:1349–60. doi: [10.1080/14737159.2021.2000393](https://doi.org/10.1080/14737159.2021.2000393)
8. Pattnaik S, Das D, Venkatesan VA, Rai A. Predicting serum hormone concentration by estimation of urinary hormones through a home-use device. *Hum Reproduction Open* 2022;2023:hoac058. doi: [10.1093/hropen/hoac058](https://doi.org/10.1093/hropen/hoac058)
9. Wegrzynowicz AK, Beckley A, Eyvazzadeh A, Levy G, Park J, Klein J. Complete Cycle Mapping Using a Quantitative At-Home Hormone Monitoring System in Prediction of Fertile Days, Confirmation of Ovulation, and Screening for Ovulation Issues Preventing Conception. *Medicina (Kaunas)*. 2022 Dec 15;58(12):1853. doi: [10.3390/medicina58121853](https://doi.org/10.3390/medicina58121853)
10. Cromack SC, Walter JR. Consumer wearables and personal devices for tracking the fertile window. *Am J Obstet Gynecol*. 2024 Nov;231(5):516-523. doi: [10.1016/j.ajog.2024.05.028](https://doi.org/10.1016/j.ajog.2024.05.028).
11. Hills E, Woodland MB, Divaraniya A. Using Hormone Data and Age to Pinpoint Cycle Day within the Menstrual Cycle. *Medicina (Kaunas)*. 2023 Jul 23;59(7):1348. doi: [10.3390/medicina59071348](https://doi.org/10.3390/medicina59071348)
12. Abdullah S, Bouchard T, Leiva R, Boehringer H, Iwaz J, Ecochard R. Distinct urinary progesterone metabolite profiles during the luteal phase. *Horm Mol Biol Clin Investig*. 2022 Dec 30;44(2):137-144. doi: [10.1515/hmbci-2022-0065](https://doi.org/10.1515/hmbci-2022-0065)
13. Direito A, Bailly S, Mariani A, Ecochard R. Relationships between the luteinizing hormone surge and other characteristics of the menstrual cycle in normally ovulating women. *Fertil Steril*. 2013 Jan;99(1):279-285.e3. doi: [10.1016/j.fertnstert.2012.08.047](https://doi.org/10.1016/j.fertnstert.2012.08.047)
14. Abdullah S, Bouchard T, Klich A, Leiva R, Pyper C, Genolini C, et al. A Quadriparametric Model to Describe the Diversity of Waves Applied to Hormonal Data. *Methods of Information in Medicine* 2018;57:101–110. doi: [10.3414/ME17-01-0102](https://doi.org/10.3414/ME17-01-0102)
15. Huo Y, Ji S, Yang H, Wu W, Yu L, Ren Y, Wang F. Differential expression of microRNA in the serum of patients with polycystic ovary syndrome with insulin resistance. *Ann Transl Med*. 2022 Jul;10(14):762. doi: [10.21037/atm-22-2941](https://doi.org/10.21037/atm-22-2941)
16. Gu Z, Hübschmann D. Make Interactive Complex Heatmaps in R. *Bioinformatics*. 2022 Feb 7;38(5):1460-1462. doi: [10.1093/bioinformatics/btab806](https://doi.org/10.1093/bioinformatics/btab806)
17. Lin W, Yang H, Lin J, Yang X, Liao Z, Zheng Y, Luo P, Liu C. OralExplorer: a web server for exploring the mechanisms of oral inflammatory diseases. *J Transl Med*. 2024 Mar 15;22(1):282. doi: [10.1186/s12967-024-05019-8](https://doi.org/10.1186/s12967-024-05019-8)
18. Dapas M, Dunaif A. Deconstructing a Syndrome: Genomic Insights Into PCOS Causal Mechanisms and Classification. *Endocr Rev*. 2022 Nov 25;43(6):927-965. doi: [10.1210/endrev/bnac001](https://doi.org/10.1210/endrev/bnac001)

19. Ecochard R, Boehringer H, Rabilloud M, Marret H. Chronological aspects of ultrasonic, hormonal, and other indirect indices of ovulation. *BJOG*. 2001 Aug;108(8):822-829. doi: [10.1111/j.1471-0528.2001.00194.x](https://doi.org/10.1111/j.1471-0528.2001.00194.x)
20. Bouchard T, Yong P, Doyle-Baker P. Establishing a Gold Standard for Quantitative Menstrual Cycle Monitoring. *Medicina (Kaunas)*. 2023 Aug 23;59(9):1513. doi: [10.3390/medicina59091513](https://doi.org/10.3390/medicina59091513)
21. Behre HM, Kuhlage J, Gassner C, Sonntag B, Schem C, Schneider HP, Nieschlag E. Prediction of ovulation by urinary hormone measurements with the home use ClearPlan Fertility Monitor: comparison with transvaginal ultrasound scans and serum hormone measurements. *Hum Reprod*. 2000 Dec;15(12):2478-82. doi: [10.1093/humrep/15.12.2478](https://doi.org/10.1093/humrep/15.12.2478)
22. Ecochard R, Guillerm A, Leiva R, Bouchard T, Direito A, Boehringer H. Characterization of follicle stimulating hormone profiles in normal ovulating women. *Fertil Steril*. 2014 Jul;102(1):237-243.e5. doi: [10.1016/j.fertnstert.2014.03.034](https://doi.org/10.1016/j.fertnstert.2014.03.034)
23. Wilcox AJ, Weinberg CR, Baird DD. Timing of sexual intercourse in relation to ovulation. Effects on the probability of conception, survival of the pregnancy, and sex of the baby. *N Engl J Med*. 1995 Dec 7;333(23):1517-21. doi: [10.1056/NEJM199512073332301](https://doi.org/10.1056/NEJM199512073332301)
24. Usala SJ, Trindade AA. A Novel Fertility Indicator Equation Using Estradiol Levels for Assessment of Phase of the Menstrual Cycle. *Medicina (Kaunas, Lithuania)* 2020;56:555. doi: [10.3390/medicina56110555](https://doi.org/10.3390/medicina56110555)
25. Ecochard R, Duterque O, Leiva R, Bouchard T, Vigil P. Self-identification of the clinical fertile window and the ovulation period. *Fertil Steril*. 2015 May;103(5):1319-25.e3. doi: [10.1016/j.fertnstert.2015.01.031](https://doi.org/10.1016/j.fertnstert.2015.01.031)
26. Bouchard TP, Schweinsberg K, Smith A, Schneider M. Using Quantitative Hormone Monitoring to Identify the Postpartum Return of Fertility. *Medicina (Kaunas)*. 2023 Nov 15;59(11):2008. doi: [10.3390/medicina59112008](https://doi.org/10.3390/medicina59112008)
27. Abdulla SH, Bouchard TP, Leiva RA, Boyle P, Iwaz J, Ecochard R. Hormonal Predictors of Abnormal Luteal Phases in Normally Cycling Women. *Front Public Health*. 2018 May 24;6:144. doi: [10.3389/fpubh.2018.00144](https://doi.org/10.3389/fpubh.2018.00144)
28. Baerwald AR, Adams GP, Pierson RA. Ovarian antral folliculogenesis during the human menstrual cycle: a review. *Hum Reprod Update*. 2012 Jan-Feb;18(1):73-91. doi: [10.1093/humupd/dmr039](https://doi.org/10.1093/humupd/dmr039)
29. Sharma A, López Y, Tsunoda T. Divisive hierarchical maximum likelihood clustering. *BMC Bioinformatics*. 2017 Dec 28;18(Suppl 16):546. doi: [10.1186/s12859-017-1965-5](https://doi.org/10.1186/s12859-017-1965-5)
30. Genolini C, Falissard B. KmL: a package to cluster longitudinal data. *Comput Methods Programs Biomed*. 2011 Dec;104(3):e112-21. doi: [10.1016/j.cmpb.2011.05.008](https://doi.org/10.1016/j.cmpb.2011.05.008)

**Correspondence to:** Thomas P. Bouchard, 108-30 Springborough Blvd SW, Calgary, Alberta, Canada, 403-667-4296

**E-mail:** [thomasbouchard@gmail.com](mailto:thomasbouchard@gmail.com)

How to cite this article: Bouchard T, Abdulla S, Leiva R, Ecochard R. Menstrual Cycle Heat Maps: Visualizing menstrual cycle variability using hormone heat map arrays referenced to the ultrasound day of ovulation, *Journal of Restorative Reproductive Medicine*. 2025 May 2. 1:4:1-9. <https://doi.org/10.63264/qk8aw674>